Available online at www.sciencedirect.com
ScienceDirect
Journal of Hazardous Materials 153 (2008) 426–433
Journal of Hazardous Materials
www.elsevier.com/locate/jhazmat

Photodegradation of 2-mercaptobenzothiazole in the γ-Fe_2O_3/oxalate suspension under UVA light irradiation

Xugang Wang [a,b], Chengshuai Liu [b], Xiaomin Li [b], Fangbai Li [b,*], Shungui Zhou [b]

[a] College of Resources and Environmental Sciences, Northwest Agriculture and Forestry University, Yangling, Shanxi 712100, PR China
[b] Guangdong Key Laboratory of Agricultural Environment Pollution Integrated Control, Guangdong Institute of Eco-Environment and Soil Science, Guangzhou 510650, PR China

Received 11 June 2007; received in revised form 24 August 2007; accepted 24 August 2007
Available online 31 August 2007

Abstract

The aim of this study is to investigate the effect of various factors on the photodegradation of organic pollutants in natural environment with co-existence of iron oxides and oxalic acid. 2-Mercaptobenzothiazole (MBT) was selected as a model pollutant, while γ-Fe_2O_3 was selected as iron oxide. The crystal structure and morphology of the prepared γ-Fe_2O_3 was determined by X-ray diffractograms (XRD) and scanning electron microscopy (SEM), respectively. The specific surface area was 14.36 m^2/g by Brunauer–Emmett–Teller (BET) method. The adsorption behavior of γ-Fe_2O_3 was evaluated by Langmuir model. The effect of the dosage of iron oxide, initial concentration of oxalic acid (C^0_{ox}), initial pH value, the light intensity and additional transition metal cations on MBT photodegradation was investigated in the γ-Fe_2O_3/oxalate suspension under UVA light irradiation. The optimal γ-Fe_2O_3 dosage was 0.4 g/L and the optimal C^0_{ox} was 0.8 mM with the UVA light intensity of 1800 mW/cm^2. And the optimal dosage of γ-Fe_2O_3 and C^0_{ox} for MBT degradation also depended strongly on the light intensity. The optimal γ-Fe_2O_3 dosage was 0.1, 0.25 and 0.4 g/L, and the optimal C^0_{ox} was 1.0, 0.8, and 0.8 mM with the light intensity of 600, 1200 and 1800 mW/cm^2, respectively. The optimal initial pH value was at 3.0. The additional transition metal cations including Cu^{2+}, Ni^{2+} or Mn^{2+} could significantly accelerate MBT degradation. This investigation will give a new insight to understanding the MBT photodegradation in natural environment.

Keywords: Photodegradation; Maghemite; Oxalate; 2-Mercaptobenzothiazole; Photo-Fenton

1. Introduction

The benzothiazole group of heterocyclic aromatic compounds is known as odorous, toxic, and poorly biodegradable pollutants in environment. 2-Mercaptobenzothiazole (MBT) is an important member of benzothiazole group and is used extensively in the manufacture of rubber as additive chemicals [1] and corrosion inhibitor [2]. A large amount of MBT enters the aquatic environment during the process of manufacture and utilization of rubber products [3]. This xenobiotic compound has been proven to be allergenic and toxic to aquatic organisms, be able to induce tumors and hamper wastewater treatment, and to inhibit degradation of degradable organic pollutants [4]. MBT has been extensively detected in wastewater effluents, sewage treatment plant and especially, in surface water. Therefore the degradation of MBT has been paid more attention in the past years [5–8]. In fact, many natural transformation processes in aquatic environment can also clear away organic pollutants. It is vital important to understand and mend these natural processes so as to achieve a faster transformation for degradation of organic pollutants in natural environment.

In fact, iron oxides and oxalic acid, which coexist together in aquatic environment, can set up a so called photo-Fenton system under light irradiation to degrade organic pollutants [9–11]. Iron is the fourth most abundant element of the earth's crust (5.1 mass%). As a kind of natural minerals and geocatalysts, iron oxides (including oxyhydroxides) are extensively found in soils, lakes and rivers, on the seafloor, and in air and organism [12]. On the other hand, oxalic acid has strong chelating ability with multivalent cations and is mainly exuded by plant roots in natural environment [13]. Oxalic acid is also an intermediate in the catalytic oxidation of phenol and coumaric acid as a byproduct of oil manufacturing [14,15]. There are iron oxides and oxalate with higher content in soils and aquatic environment.

* Corresponding author. Tel.: +86 20 87024721; fax: +86 20 87024123.
E-mail address: cefbli@soil.gd.cn (F. Li).

0304-3894/$ – see front matter © 2007 Elsevier B.V. All rights reserved.
doi:10.1016/j.jhazmat.2007.08.072

Fe(III)–oxalate exhibit strong ligand-to-metal charge transfer ability [16]. Hence, it can be expected that Fe(III)–oxalate complexes could undergo photochemical reactions in surface soil and surface water. In the past decade, several studies had reported the photochemical process of Fe(III)–oxalate and iron oxide–oxalate systems for degradation of organic pollutants [17–21]. For iron oxide–oxalate suspension system, Fe(III)–oxalate complexes includes dissolved ones and adsorbed ones [20,21]. During the photochemical reaction of Fe(III)–oxalate complexes, dissolved Fe(II) and Fe(III) species, adsorbed Fe(II) and Fe(III) species, the superoxides and hydroperoxyl radicals ($O_2^{\bullet-}$/$^{\bullet}$OOH) are the key intermediates formed through the reactions, as shown in Eqs. (1)–(6). H_2O_2 can be obtained by the dismutation of $O_2^{\bullet-}$/$^{\bullet}$OOH, as Eqs. (7) and (8). After H_2O_2 was formed, the classical Fenton reaction happened with Fe(II) species, the photo-reduction products of Fe(III) species, to form $^{\bullet}$OH, as Eq. (9). In our previous investigation, the formation of H_2O_2 had been confirmed [21].

$$\text{Iron oxide} + nH_2C_2O_4 \leftrightarrow [\equiv Fe(C_2O_4)_n]^{(2n-3)-} \quad (1)$$

$$[\equiv Fe(C_2O_4)_n]^{(2n-3)-} + h\nu \rightarrow Fe(C_2O_4)_2{}^{2-} \text{ (or } \equiv Fe(C_2O_4)_2{}^{2-}) + (C_2O_4)^{\bullet-} \quad (2)$$

$$Fe^{III}(C_2O_4)_n{}^{3-2n} + h\nu \rightarrow [Fe^{II}(C_2O_4)_{(n-1)}]^{4-2n} + (C_2O_4)^{\bullet-} \quad (3)$$

$$(C_2O_4)^{\bullet-} \rightarrow CO_2 + CO_2{}^{\bullet-} \quad (4)$$

$$CO_2{}^{\bullet-} + O_2 \rightarrow CO_2 + O_2{}^{\bullet-} \quad (5)$$

$$O_2{}^{\bullet-} + H^+ \rightarrow {}^{\bullet}OOH \quad (6)$$

$$O_2{}^{\bullet-} + Fe^{3+} \rightarrow Fe^{2+} + O_2 \quad (7)$$

$$O_2{}^{\bullet-}/{}^{\bullet}OOH + nH^+ + Fe^{2+} \rightarrow Fe^{3+} + H_2O_2 \quad (8)$$

$$Fe^{2+} + H_2O_2 \rightarrow Fe^{3+} + OH^- + {}^{\bullet}OH \quad (9)$$

Generally, organic pollutants could be degraded efficiently by hydroxyl radical ($^{\bullet}$OH) with high oxidation potential, produced in the above-mentioned photo-Fenton system. However, the photodegradation of MBT in iron oxide–oxalate system is a function of various factors including the dosage of iron oxide, initial concentration of oxalic acid (C_{ox}^0), initial pH value, irradiated light intensity and additional transition metal cations which may coexist with organic pollutants. And to our best knowledge, there was little literature reporting the effect of these factors on MBT photodegradation.

In this study, maghemite (γ-Fe_2O_3) was home prepared to conduct MBT degradation experiments in the presence of oxalic acid in order to have a better understanding of the photodegradation of organic pollutants in aquatic environment with existence of iron oxides and oxalic acids. Maghemite is employed here as the representative iron oxide because it exists in soils and surface water in tropical and subtropical regions [12]. The objectives of this study are to investigate the effects of above-mentioned factors on MBT degradation and then to understand the photodegradation of organic pollutants in natural environment with co-existence of iron oxides and oxalic acid.

2. Experimental

2.1. Reagents

2-Mercaptobenzothiazole (MBT) with analytical grade was purchased from Sigma–Aldrich (St. Louis, MO, USA). Other chemicals with analytical grades were purchased from Guangzhou Chemical Co., China. All the chemicals were used without further purification and all solutions were prepared with deionized water.

2.2. Preparation and characterization of γ-Fe_2O_3

The γ-Fe_2O_3 was prepared by hydrothermal method. First, 500 mL of 0.2 M $FeCl_2$ solution, 100 mL of 2 M $(CH_2)_6N_4$ solution, and 100 mL of 1.25 M $NaNO_3$ solution were mixed to obtain a black green precipitate. And then the precipitate was aged in the mixture at 80 °C for 6 h before it was filtered by 0.45 μm glass fiber paper. The precipitate remained on the filter paper was washed three times with alcohol and distilled water to remove anions and organic impurities and then dried at 60 °C for 60 h. The dried gel was ground and γ-Fe_2O_3 powders were obtained. The X-ray powder diffraction patterns of γ-Fe_2O_3 was recorded on a Rigaku D/Max-III A diffract meter at room temperature, operating at 30 kV and 30 mA, using a Cu Kα radiation ($\lambda = 0.15418$ nm). The specific surface area of γ-Fe_2O_3 was measured by the Brunauer–Emmett–Teller (BET) method in which the N_2 adsorption at 77 K was applied and Carlo Erba Sorptometer was used [22]. The surface morphology of γ-Fe_2O_3 was observed using scanning electron microscopy (SEM Leica Stereoscan 400i series).

2.3. Adsorption isotherm experiment

Adsorption of MBT on γ-Fe_2O_3 was determined by using the batch experiment in the dark. A fixed amount of γ-Fe_2O_3 (0.10 g) was added to 10 mL of MBT solution with varying concentrations in glass tubes, which were sealed and agitated for 24 h at 200 rpm in a thermostatic shaker bath and maintained at a temperature of 25 ± 1 °C. The concentrations of MBT after adsorbed were measured by liquid chromatography and the adsorbed amount of MBT on γ-Fe_2O_3 was calculated based on a mass balance.

2.4. Set up of photochemical reactor

All photoreaction experiment were carried out in a photochemical reactor system, which consisted of a Pyrex cylindrical reactor vessel with an effective volume of 250 mL, a cooling water jacket, two aeration inlet in the foot, and UVA lamps

(Luzchem Research, Inc.) positioned axially at the center as a UVA light source with different light intensity at the main emission of 365 nm. The glass in outer shell of the reactor was Pyrex, while the glass between the vessel and the lamp was quartz. The reaction temperature was kept at 25 ± 1 °C by cooling water, and the reaction suspension was constant stirred on a magnetically stirrer during the reaction process. The intensity of the light was measured by a UVA radiation meter (Photoelectric Instrument Factory of Beijing Normal University) with a sensor of 365 nm wavelength. The radio meter was set up at the same position of the reactor when tested.

2.5. Photochemical experimental procedure

The reaction suspension was prepared by adding given dosage of γ-Fe_2O_3 powder into 250 mL of aqueous MBT solution or mixed MBT and oxalic acid solution. Prior to photoreaction, the suspension was magnetically stirred in a dark condition for 30 min to establish an adsorption/desorption equilibrium status. The aqueous reaction suspension was then irradiated under UVA light with constant aeration, with the dissolved oxygen concentration of 11.84 mg/L, which measured by a dissolved oxygen meter, Model 9173R from Shanghai Hong Ji Instrument Ltd., China. At given time intervals, the analytical samples were taken from the suspension and immediately centrifuged at 4500 rpm for 20 min. The supernatant was carefully transferred and stored in the dark for analysis. In these experiments, the initial concentrations of MBT were 10 mg/L and the initial pH values were not been adjusted unless otherwise stated.

2.6. Analytical method

The remaining MBT after the adsorption and during the photodegradation was determined by high performance liquid chromatography (HPLC). A mobile phase consisting of 70% methanol (HPLC grade) and 30% water (HPLC grade) acidified by adding 1% (v/v) acetic acid was operated at a flow rate of 0.5 mL/min, and a wavelength of 323 nm was used to detect MBT. The concentration of Fe^{3+} and Fe^{2+} ions were tested by the 1,10-phenanthroline method [23].

3. Results and discussion

3.1. Properties of γ-Fe_2O_3

Fig. 1 showed the standard XRD of γ-Fe_2O_3 and XRD graph of the prepared iron oxide. The result showed that γ-Fe_2O_3 powder was obtained because all seven peaks of (2 2 0), (3 1 1), (2 2 2), (4 0 0), (4 2 2), (5 1 1) and (4 4 0) determined by XRD were attributable to γ-Fe_2O_3 [24]. The average crystal size of γ-Fe_2O_3 was 43.2 nm deduced from Scherrer formula with its strongest XRD peak [25]. The specific surface area of γ-Fe_2O_3 was 14.36 m^2/g and the total pore volume was 0.05 cm^3/g, measured by BET–BJH method. The morphology was examined by SEM, as shown in Fig. 2, indicating that the porous structure was attributed to the pores formed between iron oxides particles. SEM photo showed the shape of γ-Fe_2O_3 was uniformity of spherical.

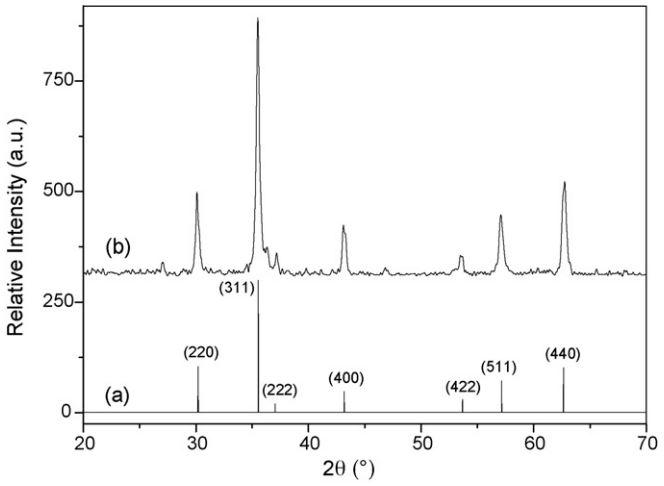

Fig. 1. The standard XRD graph of γ-Fe_2O_3 (a) and XRD graph of prepared powder (b).

3.2. The adsorption behavior of γ-Fe_2O_3

The adsorption isotherm of MBT on γ-Fe_2O_3 was shown in Fig. 3, which was well fitted by the Langmuir adsorption model as Eq. (10)

$$\frac{C_e}{\Gamma} = \frac{1}{\Gamma_{max}} C_e + \frac{1}{K_a \Gamma_{max}} \quad (10)$$

where C_e is the equilibrium concentration in the solution in mM, K_a the adsorption equilibrium constant in L/mol, and Γ_{max} is the saturated adsorption capacity in mol/g. The saturated adsorption amount (Γ_{max}) of MBT onto γ-Fe_2O_3 was 3.87×10^{-5} mol/g and the adsorption equilibrium constant (K_a) was 25.01 L/mol with the correlative coefficient R of 0.9974.

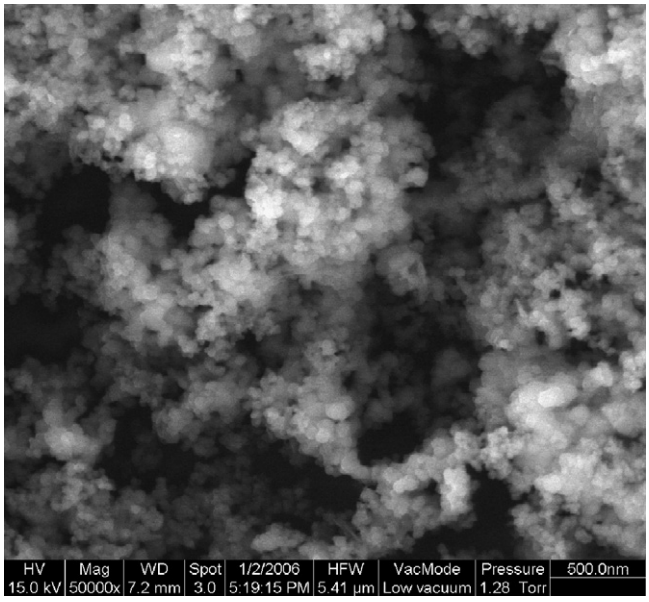

Fig. 2. The SEM photograph of γ-Fe_2O_3 powder.

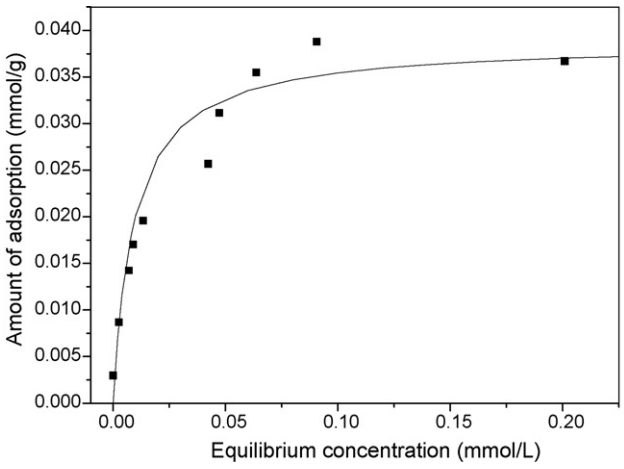

Fig. 3. The adsorption isotherm of MBT on the surface of γ-Fe_2O_3 obtained by plotting the equilibrium concentration (C_e) vs. the adsorbed amounts of MBT (Γ).

3.3. Photodegradation of MBT in the γ-Fe_2O_3/oxalate suspension

Fig. 4 showed the photodegradation of MBT with the initial concentration of 10 mg/L under different conditions. Without oxalic acid but only with 0.4 g/L γ-Fe_2O_3 under 1800 mW/cm^2 UVA light irradiation (curve a), the degradation of MBT was almost negligible. However, when 0.8 mM oxalic acid was presented with the same condition as curve a, the rate of MBT degradation was obviously enhanced and the removal of MBT was 96.7% after 45 min (curve b). In iron oxide suspension, oxalic acid is first adsorbed on the surface of γ-Fe_2O_3 to form iron oxide–oxalate complexes of $[\equiv Fe^{III}(C_2O_4)_n]^{3-2n}$ (Eq. (1)). $[\equiv Fe^{III}(C_2O_4)_n]^{3-2n}$ on the surface or $Fe^{III}(C_2O_4)_n{}^{3-2n}$ in the solutions [26] can be excited to form $[\equiv Fe^{II}(C_2O_4)_{(n-1)}]^{4-2n}$ and oxalate radical $(C_2O_4)^{\bullet -}$ as described by Eqs. (2) and (3), and the oxalate radical can easily be transferred into carbon-centered radical $(CO_2)^{\bullet -}$ (Eq. (4)). Then the excited electron is transferred from carbon-centered radical into adsorbed oxygen forming superoxide ion ($O_2^{\bullet -}$) as described by Eq. (5). Fe(III) can react with $O_2^{\bullet -}$ to form O_2 and Fe(II), and Fe(II) reacts with $O_2^{\bullet -}$ and $^{\bullet}OOH$ to form H_2O_2 in acidic solution with Fe(III) (Eqs. (7) and (8)). To be important, Fe(II) is re-oxidized to Fe(III) in the presence of O_2. After H_2O_2 was formed, hydroxyl radical ($^{\bullet}OH$) could be generated by the reaction of Fe(II) with H_2O_2 as described by Eq. (9). The formation of $^{\bullet}OH$ during the photochemical process of Fe(II)–oxalate system had been reported [27]. And, the formation of H_2O_2 had been determined in our previous work [21]. The co-existence Fe(II) and H_2O_2 could imply the formation of $^{\bullet}OH$ under UVA light irradiation. The hydroxyl radical, which has strong oxidation potential, can effectively oxidize MBT. It should be noted that this photochemical process happened both on the surface of γ-Fe_2O_3 as a heterogeneous photo-Fenton reaction and in the solution as a homogeneous one. To compare the efficiency in γ-Fe_2O_3–oxalate system with that in Fe(III)–oxalate homogeneous system, a homogeneous system was set up by adding 0.06 mM Fe^{3+} (the same concentration in γ-Fe_2O_3–oxalate suspension) and 0.8 mM C_{ox}^0 to degrade MBT under 1800 mW/cm^2 UVA irradiation, as shown by curve c in Fig. 4. The results showed that the removal of MBT was only 50%, much lower than that in curve b. This implied that the degradation of MBT in γ-Fe_2O_3–oxalate system should be achieved by both heterogeneous and homogeneous photo-Fenton reactions.

3.4. The effect of γ-Fe_2O_3 dosage

Fig. 5 showed the dependence of MBT degradation on the dosage of γ-Fe_2O_3 in the presence of 1.0 mM oxalic acid under irradiation of 1800 mW/cm^2 UVA light. The photodegradation of MBT in γ-Fe_2O_3/oxalate system can be described well by first-order kinetic and the first-order reaction kinetic constant (k) versus the dosage of γ-Fe_2O_3 was plotted as the

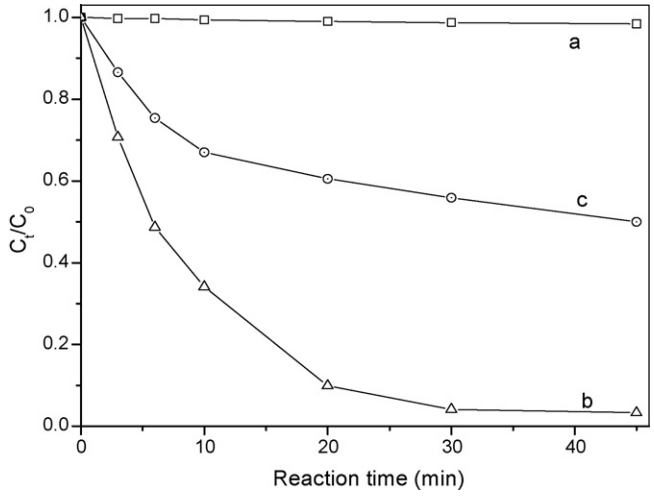

Fig. 4. The photodegradation of 10 mg/L MBT under UVA irradiation with the intensity of 1800 mW/cm^2 in 250 mL solutions with (a) 0.4 g/L γ-Fe_2O_3; (b) 0.4 g/L γ-Fe_2O_3 + 0.8 mM C_{ox}^0; (c) 0.06 mM Fe^{3+} + 0.8 mM C_{ox}^0.

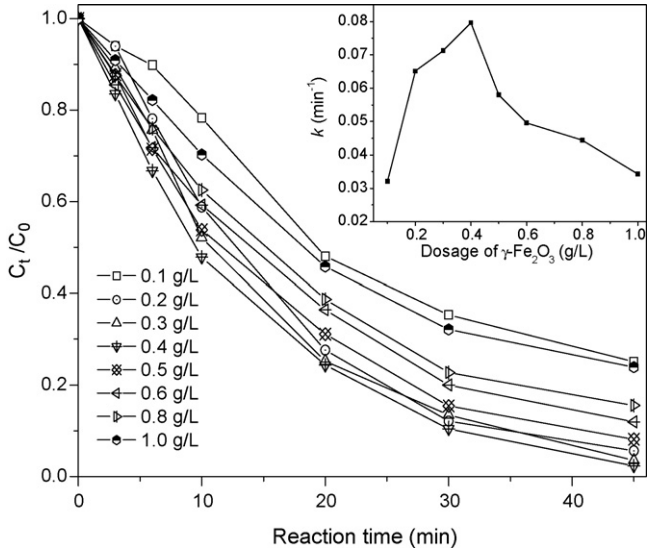

Fig. 5. The effect of γ-Fe_2O_3 dosage on the photodegradation of 10 mg/L MBT with the light intensity of 1800 mW/cm^2 in the presence of 1.0 mM C_{ox}^0 (the inserted figure presents the dependence of k on the dosage of iron oxide).

inserted figure of Fig. 4. The first-order kinetic constants k were 3.21×10^{-2} ($R = 0.9922$), 6.51×10^{-2} ($R = 0.9858$), 7.13×10^{-2} ($R = 0.9854$), 7.96×10^{-2} ($R = 0.9908$), 5.80×10^{-2} ($R = 0.9886$), 4.96×10^{-2} ($R = 0.9830$), 4.44×10^{-2} ($R = 0.9830$) and $3.43 \times 10^{-2}\,\text{min}^{-1}$ ($R = 0.9867$) when the dosages of γ-Fe_2O_3 were 0.10, 0.20, 0.30, 0.40, 0.50, 0.60, 0.80 and 1.00 g/L, respectively. Obviously, there should be an optimal dosage of 0.40 g/L γ-Fe_2O_3 for MBT degradation. The γ-Fe_2O_3 acted as a heterogeneous catalyst that can significantly accelerate the formation of $[\equiv Fe^{III}(C_2O_4)_n]^{3-2n}$ which had high photoactivity. And under UVA irradiation, $^{\bullet}OH$ can be produced more during the photochemical reaction of $[\equiv Fe^{III}(C_2O_4)_n]^{3-2n}$ with more γ-Fe_2O_3 as stated in Section 3.3. On the other hand, the reaction suspension became more turbid with an excessive γ-Fe_2O_3 loading, so as to inhibit the penetration of UVA light and decrease the formation of $^{\bullet}OH$. Therefore, the photodegradation of MBT in γ-Fe_2O_3/oxalate system depended strongly on the dosage of iron oxide and an optimal dosage of γ-Fe_2O_3 was 0.4 g/L, at which the first-order kinetic constant (k) reached the maximal value of $7.96 \times 10^{-2}\,\text{min}^{-1}$.

3.5. The effect of initial concentration of oxalic acid (C_{ox}^0)

Fig. 6 showed the dependence of MBT photodegradation on the C_{ox}^0 with 0.4 g/L γ-Fe_2O_3 under 1800 mW/cm^2 UVA light irradiation, and the inserted figure presented the dependence of the first-kinetic constant (k) on the C_{ox}^0. The results showed that the photodegradation of MBT almost did not occur in the absence of oxalic acid (curve 0.0 mM). However, MBT degradation could be efficiently enhanced in the presence of oxalic acid. The first-order kinetic constant (k) for MBT degradation increased with increasing C_{ox}^0 from 0.0 to 0.8 mM, at which k reached $8.98 \times 10^{-2}\,\text{min}^{-1}$. However, the first-order kinetic constant for MBT degradation decreased when the C_{ox}^0 was over 0.8 mM and the k values were 6.75×10^{-2}, 5.03×10^{-2}, 3.07×10^{-2} and $2.89 \times 10^{-2}\,\text{min}^{-1}$ when the C_{ox}^0 was up to 1.0, 1.2, 1.6 and 2.0 mM, respectively. The results stationed above indicated that C_{ox}^0 should be a vital factor in γ-Fe_2O_3/oxalate system for MBT degradation. However, excessive oxalic acid would occupy the adsorbed sites on the surface of iron oxide and also react competitively with generated hydroxyl radical together with MBT. The adsorption of MBT on the surface would also be hindered and only a part of hydroxyl radical would be utilized by MBT. Furthermore, excessive oxalic acid would lead to the formation of a large amount of Fe^{3+}, which would inhibit the formation of H_2O_2 as indicated by Eq. (7). Therefore, the optimal C_{ox}^0 in γ-Fe_2O_3/oxalate system was 0.8 mM which mostly favored the photodegradation of MBT in the system.

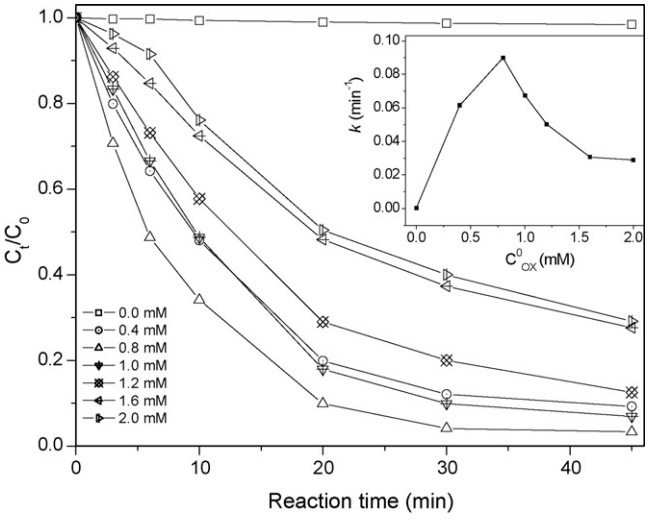

Fig. 6. The effect of initial concentration of oxalic acid (C_{ox}^0) on the photodegradation of 10 mg/L MBT with the light intensity of 1800 mW/cm^2 with 0.4 g/L γ-Fe_2O_3 (the inserted figure presents the dependence of k on the C_{ox}^0).

3.6. The effect of UVA light intensity

Light intensity is another important factor to be considered during photochemical process, especially in natural environment. Generally, higher light intensity can lead to a higher degradation rate for organic pollutants in photochemical reaction. The same results were obtained in this investigation as shown in Fig. 7. However, the more interesting results obtained here were that the light intensity might influence the dependence of k value on the dosage of γ-Fe_2O_3 and on the C_{ox}^0. A series of experiments were carried out to investigate the effect of the light intensity on the optimal dosage of γ-Fe_2O_3. The dependence of k values for the degradation of 10 mg/L MBT on the dosage of γ-Fe_2O_3 and on the UVA light intensity in the presence of 1.0 mM C_{ox}^0 was shown in Fig. 7(A). The results indicated that the k values should increase obviously with different dosages of γ-Fe_2O_3 and the optimal dosage of γ-Fe_2O_3 should increase significantly with the increase of UVA light intensity. It was extensively reported that the increase of the light intensity can enhance the rate of reaction by increasing the number of charge carriers for semiconductor catalyst [28]. For the iron oxide/oxalate system, the increase of the light intensity can accelerate the photochemical reaction rate by increasing the rate of the photo-reduction of $[\equiv Fe^{III}(C_2O_4)_n]^{3-2n}$ to form Fe(II) species which can react with H_2O_2, and then to enhance the production of $^{\bullet}OH$. On the other hand, the optimal dosages of γ-Fe_2O_3 were 0.10, 0.25 and 0.40 g/L with the k values of 2.81×10^{-2}, 6.46×10^{-2} and $7.96 \times 10^{-2}\,\text{min}^{-1}$ for MBT degradation under the UVA light intensity of 600, 1200 and 1800 mW/cm^2, respectively. Generally, more γ-Fe_2O_3 was needed to form $[\equiv Fe^{III}(C_2O_4)_n]^{3-2n}$ to be exited with the increase in the UVA light intensity.

A series of experiments were also carried out to investigate the effect of the light intensity on the C_{ox}^0. Fig. 7(B) showed that the dependence of k values for the degradation of 10 mg/L MBT on the C_{ox}^0 with the optimal dosage of 0.10, 0.25 and 0.40 g/L γ-Fe_2O_3 under the UVA light intensity of 600, 1200 and 1800 mW/cm^2, respectively. The results showed that the UVA light intensity could also affect the optimal C_{ox}^0. The optimal C_{ox}^0 was 1.0 mM under the light intensity of 600 or 1200 mW/cm^2, while the optimal C_{ox}^0 decreased to 0.8 mM under the light intensity of 1800 mW/cm^2. That indicated that the increase of UVA light intensity could accelerate

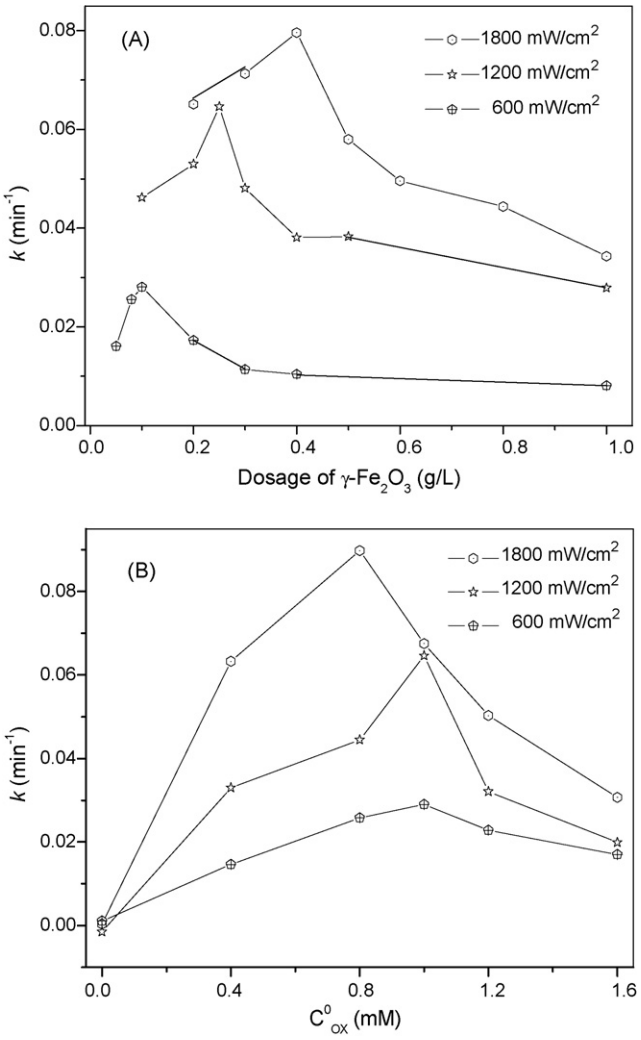

Fig. 7. The dependence of first-order kinetic constants (k) for 10 mg/L MBT degradation on the dosage of γ-Fe_2O_3 in the presence of 1.0 mM C^0_{ox} with the UVA light intensity of 600, 1200, 1800 mW/cm^2 (A), and the dependence of first-order kinetic constants (k) for 10 mg/L MBT degradation on the C^0_{ox} with the intensity of 600, 1200, 1800 mW/cm^2 with the optimal dosage of γ-Fe_2O_3 (B).

the photo-reduction of $[\equiv Fe^{III}(C_2O_4)_n]^{3-2n}$ and the formation of $^{\bullet}$OH.

3.7. The effect of initial pH

It has been reported that the optimal initial pH value might be at about 3 for organic pollutants degradation in the homogeneous photo-Fenton reaction [29,30]. In this investigation, the effect of initial pH value on MBT degradation in γ-Fe_2O_3/oxalate system was also studied in the initial pH interval range from 2 to 11. Fig. 8 showed the dependence of k value for MBT degradation on the initial pH in γ-Fe_2O_3/oxalate system, which adjusted by titrating NaOH or HCl before reaction, in the presence of 0.4 g/L γ-Fe_2O_3 and 0.8 mM C^0_{ox} under 1800 mW/cm^2 UVA light intensity. The results showed that the optimal initial pH value should be around 3.0, at which the k value for MBT degradation was 9.05×10^{-2} min^{-1}. The γ-Fe_2O_3/oxalate system at initial pH 3.0 might have a higher concentration of $[\equiv Fe^{III}(C_2O_4)_n]^{3-2n}$,

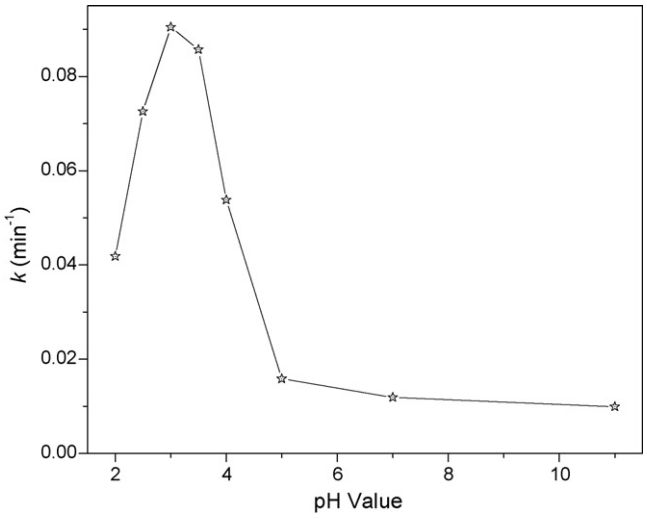

Fig. 8. The dependence of first-order kinetic constants (k) for 10 mg/L MBT degradation on the initial pH (the reaction systems contained 0.4 g/L γ-Fe_2O_3 and 0.8 mM C^0_{ox} under 1800 mW/cm^2 UVA light irradiation).

and then more $^{\bullet}$OH generation would be generated [18]. When the pH value increased to 4–5, ≡Fe(III)–oxalate species were mainly $\equiv Fe^{III}(C_2O_4)^+$, which is low photoactive. And especially, when the pH value was above 5, the predominant Fe(III) and Fe(II) species were ≡Fe(II)–OH and ≡Fe(III)–OH as the precipitate, which might hardly be photoactive. At lower initial pH 2, the dissolution of γ-Fe_2O_3 by H^+ was excessive and the complex of γ-Fe_2O_3 and oxalate was hindered, and less $[\equiv Fe^{III}(C_2O_4)_n]^{3-2n}$ on the surface of γ-Fe_2O_3 was formed, so as to decrease the yields of $^{\bullet}$OH, then leading to a lower rate of MBT degradation.

3.8. Effect of additional transition metal cations

Cu^{2+}, $Ni^{2+}$and Mn^{2+}, which are prevalent metal pollutants that exist in natural environment, may induce the compound pollution with organic pollutants [31,32]. It is mostly interesting to study the effect of these trace cations on the degradation of organic pollutants in γ-Fe_2O_3/oxalate system. The experiments were conducted to degrade 10 mg/L MBT with 0.4 g/L γ-Fe_2O_3 and 0.8 mM C^0_{ox}, in the presence of 50 μM transition metal cations under 1800 mW/cm^2 UVA light irradiation. The effects of different transition metal cations on MBT degradation were showed in Fig. 9 and the k values were shown in the inserted figure. The results showed that the additional Cu^{2+}, Ni^{2+} or Mn^{2+} could enhance the photodegradation of MBT significantly. The k value was 8.98×10^{-2} min^{-1} when without any transition metal cations while that increased significantly up to 13.01×10^{-2} ($R = 0.9661$), 11.26×10^{-2} ($R = 0.9536$) and 10.84×10^{-2} ($R = 0.9406$) min^{-1} in the presence of 50 μM Cu^{2+}, Ni^{2+} or Mn^{2+}, respectively. The enhanced effect of additional transition metal cations could be explained in the following ways: (1) the transition metal cations can act as charge carrier and also can complex with oxalic acid to form the M-oxalate complexes which can participate in the photochemical process [33,34], as shown in Eq. (11), where M was represented

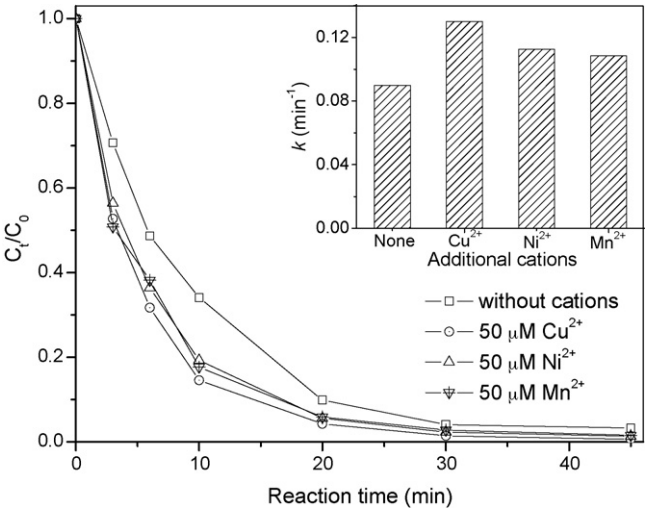

Fig. 9. The effects of additional transition metal cations, Cu^{2+}, Ni^{2+} or Mn^{2+} with the concentration of 50 μM, on the photodegradation of 10 mg/L MBT with the UVA light intensity of 1800 mW/cm^2 in the presence of 0.8 mM C_{ox}^0 (the inserted figure showed the k values for MBT degradation with different additional cations).

as the transition metal and (2) transition metal cations can also act as the substitute for Fe(II) species which reacting with H_2O_2, even conducting a faster reaction rate to form a so called Fenton-like reaction [35,36]. The presence of transition metal cations can also increase the utility efficiency of oxalic acid to form more $^{\bullet}$OH and decrease the competitively reaction with $^{\bullet}$OH for MBT degradation.

$$M^{2+} + nH_2C_2O_4 \leftrightarrow [M(C_2O_4)_{(n-1)}]^{4-2n} \quad (11)$$

4. Conclusions

MBT degradation depended significantly on various factors including the dosage of iron oxide, initial concentration of oxalic acid (C_{ox}^0), initial pH value, the light intensity and additional transition metal cations in γ-Fe_2O_3/oxalate system under UVA light irradiation. The optimal γ-Fe_2O_3 dosage was 0.4 g/L and the optimal C_{ox}^0 was 0.8 mM with UVA light intensity at 1800 mW/cm^2. And the optimal dosage of γ-Fe_2O_3 and the optimal C_{ox}^0 for MBT degradation also depended strongly on the light intensity. The optimal initial pH was at 3.0. The additional transition metal cations including Cu^{2+}, Ni^{2+} or Mn^{2+} could accelerate MBT degradation significantly.

Acknowledgments

The work was financially supported by the National Natural Science Foundation of PR China (No. 20377011) and the Natural Science Foundation Key Project of Guangdong province (No. 036533).

References

[1] H.W. Engels, H.J. Weidenhaupt, M. Abele, M. Pieroth, W. Hofmann, Ullmann's Encyclopedia of Industrial Chemistry, vol. 112, fifth ed., Wiley-VCH, Weinheim, 1993.
[2] C.C. Chen, C.E. Lin, Analysis of copper corrosion inhibitors by capillary zone electrophoresis, Anal. Chim. Acta 321 (1996) 215–218.
[3] Anon, 2-Mercaptobenzothiazole; proposed test rule, Federal Register 50 (1985) 46121.
[4] O. Fiehn, G. Wegener, J. Jochimshn, M. Jekel, Analysis of the ozonation of 2-mercaptobenzothiazole in water and tannery wastewater using sum parameters, liquid- and gas chromatography and capillary electrophoresis, Water Res. 32 (1998) 1075–1084.
[5] M.H. Habibi, S. Tangestaninejad, B. Yadollahi, Photocatalytic mineralisation of mercaptans as environmental pollutants in aquatic system using TiO_2 suspension, Appl. Catal. B: Environ. 33 (2001) 57–63.
[6] F.B. Li, X.Z. Li, M.F. Hou, Photocatalytic degradation of 2-mercaptobenzothiazole in aqueous La^{3+}–TiO_2 suspension for odor control, Appl. Catal. B: Environ. 48 (2004) 185–194.
[7] M.A. Malouki, C. Richard, A. Zertal, Photolysis of 2-mercaptobenzothiazole in aqueous medium: laboratory and field experiments, J. Photochem. Photobiol. A: Chem. 167 (2004) 121–126.
[8] F.B. Li, X.Z. Li, K.H. Ng, Photocatalytic degradation of an odorous pollutant: 2-mercaptobenzothiazole in aqueous suspension using Nd^{3+}–TiO_2 catalysts, Ind. Eng. Chem. Res. 45 (2006) 1–7.
[9] C. Siffert, B. Sulzberger, Light-induced dissolution of hematite in the presence of oxalate. A case study, Langmuir 7 (1991) 1627–1634.
[10] B.C. Faust, J. Allen, Photochemistry of aqueous iron(III)–polycarboxylate complexes: roles in the chemistry of atmospheric and surface waters, Environ. Sci. Technol. 27 (1993) 2517–2522.
[11] Y.G. Zuo, Y.W. Deng, Iron(II)-catalyzed photochemical decomposition of oxalic acid and generation of H_2O_2 in atmospheric liquid phases, Chemosphere 35 (1997) 2051–2058.
[12] R.M. Cornell, U. Schwertmann, The Iron Oxides: Structure, Properties, Reactions, Occurrences and Uses, 2nd ed., Wiley-VCH, Weinheim, 2003.
[13] T. Kayashima, T. Katayama, Oxalic acid is available as a natural antioxidant in some systems, Biochim. Biophys. Acta: Gen. Subj. 1573 (2002) 1–3.
[14] H. Kušić, N. Koprivanac, A.L. Božić, S. Selanec, Photo-assisted Fenton type processes for the degradation of phenol: a kinetic study, J. Hazard. Mater. B136 (2006) 632–644.
[15] X.L. Hao, M.H. Zhou, L.C. Lei, Non-thermal plasma-induced photocatalytic degradation of 4-chlorophenol in water, J. Hazard. Mater. B141 (2007) 475–482.
[16] G. Sposito, The Surface Chemistry of Soils, Oxford University Press, Oxford, UK, 1989.
[17] V. Nadtochenko, J.J. Kiwi, Photoinduced adduct formation between orange II and [Fe^{3+}(aq)] or $Fe(ox)_3^{3-}$–H_2O_2 photocatalytic degradation and laser spectroscopy, J. Chem. Soc., Faraday Trans. 93 (1997) 2373–2378.
[18] M.E. Balmer, B. Sulzberger, Atrazine degradation in irradiated iron/oxalate system systems: effects of pH and oxalate, Environ. Sci. Technol. 33 (1999) 2418–2424.
[19] P. Mazellier, B. Sulzberger, Diuron degradation in irradiated, heterogeneous iron/oxalate systems: the rate-determining step, Environ. Sci. Technol. 35 (2001) 3314–3320.
[20] J. Lei, C. Liu, F. Li, X. Li, S. Zhou, X. Liu, G. Ming, Q. Wu, Photodegradation of orange I in the heterogeneous iron oxide–oxalate complex system under UVA irradiation, J. Hazard. Mater. B137 (2006) 1016–1024.
[21] F.B. Li, X.Z. Li, X.M. Li, T.X. Liu, J. Dong, Heterogeneous photodegradation of bisphenol A with iron oxides and oxalate in aqueous solution, J. Colloid Interface Sci. 311 (2007) 481–490.
[22] J.G. Yu, J.C. Yu, M.K.-P. Leung, W.K. Ho, B. Cheng, X.J. Zhao, J.C. Zhao, Effects of acidic and basic hydrolysis catalysts on the photocatalytic activity and microstructures of bimodal mesoporous titania, J. Catal. 217 (2003) 69–78.
[23] C. Paipa, M. Mateo, I. Godoy, E. Poblete, M.I. Toral, T. Vargas, Comparative study of alternative methods for the simultaneous determination of Fe^{+3} and Fe^{+2} in leaching solutions and in acid mine drainages, Miner. Eng. 18 (2005) 1116–1119.
[24] K. Woo, J. Hong, S. Choi, H.-W. Lee, J.-P. Ahn, C.S. Kim, S.W. Lee, Easy synthesis and magnetic properties of iron oxide nanoparticles, Chem. Mater. 16 (2004) 2814–2818.

[25] J. Yu, S. Liu, H. Yu, Microstructures and photoactivity of mesoporous anatase hollow microspheres fabricated by fluoride-mediated self-transformation, J. Catal. 249 (2007) 59–66.
[26] Y. Chen, F. Wu, Y. Lin, N. Deng, N. Bazhin, E. Glebov, Photodegradation of glyphosate in the ferrioxalate system, J. Hazard. Mater. B 148 (2007) 360–365.
[27] J.H. Ma, W.H. Ma, W.J. Song, C.C. Chen, Y.L. Tang, J.C. Zhao, Fenton degradation of organic pollutants in the presence of low-molecular-weight organic acids: cooperative effect of quinine and visible light, Environ. Sci. Technol. 40 (2006) 618–624.
[28] H.M. Coleman, M.I. Abdullah, B.R. Eggins, F.L. Palmer, Photocatalytic degradation of 17β-oestradiol, oestriol and 17α-ethynyloestradiol in water monitored using fluorescence spectroscopy, Appl. Catal. B: Environ. 55 (2005) 23–30.
[29] B.D. McGinnis, V.D. Adams, E.J. Middlebrooks, Degradation of ethylene glycol in photo Fenton systems, Water Res. 34 (2000) 2346–2354.
[30] X.-K. Zhao, G.-P. Yang, Y.-J. Wang, X.-Ch. Gao, Photochemical degradation of dimethyl phthalate by Fenton reagent, J. Photochem. Photobiol. A: Chem. 161 (2004) 215–220.
[31] R. Mandal, A.L.R. Sekaly, J. Murimboh, N.M. Hassan, C.L. Chakrabarti, M.H. Back, D.C. Grégoire, W.H. Schroeder, Effect of the competition of copper and cobalt on the lability of Ni(II)–organic ligand complexes, Part II: in freshwaters (Rideau River surface waters), Anal. Chim. Acta 395 (1999) 323–334.
[32] A. Binelli, F. Ricciardi, C. Riva, A. Provini, Screening of POP pollution by AChE and EROD activities in Zebra mussels from the Italian Great Lakes, Chemosphere 61 (2005) 1074–1082.
[33] M. Louloudi, K. Mitopoulou, E. Evaggelou, Y. Deligiannakis, N. Hadjiliadis, Homogeneous and heterogenized copper(II) complexes as catechol oxidation catalysts, J. Mol. Catal. A: Chem. 198 (2003) 231–240.
[34] J.-K. Wang, Preferential transport behaviors of ternary system ferric-cupric-nickel ions through cation ion exchange membrane with a complex agent by dialysis, Desalination 161 (2004) 277–285.
[35] T. Kowalik-Jankowska, M. Ruta, K. Wisniewska, L. Lankiewicz, M. Dyba, Preferential transport behaviors of ternary system ferric-cupric-nickel ions through cation ion exchange membrane with a complex agent by dialysis, J. Inorg. Biochem. 98 (2004) 940–950.
[36] S. Irmak, H.I. Yavuz, O. Erbatur, Degradation of 4-chloro-2-methylphenol in aqueous solution by electro-Fenton and photoelectro-Fenton processes, Appl. Catal. B: Environ. 63 (2006) 243–248.